HIERBATCHING: LOCALITY-AWARE OUT-OF-CORE TRAINING OF GRAPH NEURAL NETWORKS

Anonymous authors
Paper under double-blind review

ABSTRACT

Graph neural networks (GNNs) have become increasingly popular for analyzing data organized as massive graphs. Efficient training of GNN models under limited computing resources is critical for GNN's widespread adoption. We consider the use of a single commodity machine with limited memory (e.g., 128GB) but ample external storage (e.g., 1TB). On such a platform, the feature data or even the graph may not fit in the memory. When data is stored on external storage, gathering features and constructing neighborhood subgraphs in a typical mini-batch training incurs random storage accesses and thus, causes expensive data movement.

To overcome this bottleneck, we propose a *locality-aware* training scheme, coined HierBatching, which significantly increases training speed while retaining the training quality. The key idea is to exploit the memory hierarchy of a modern GPU machine by constructing batches in an analogously hierarchical manner. HierBatching groups nodes in partitions, each of which is laid out contiguously in the disk for maximal *spatial locality*. Meanwhile, the main memory is treated as a cache that holds a mega-batch, which is a random collection of partitions. Mini-batches are sampled for GPU training from the mega-batch in the main memory. Each mega-batch is reused multiple times to improve *temporal locality*. Our experiments show that on a machine with 128GB main memory, HierBatching is **3**× to **20**× faster than a straightforward out-of-core training approach by using mmap, while maintaining the prediction accuracy.

1 INTRODUCTION

Graph neural networks (GNNs) have emerged as effective machine learning models for many practical applications, such as social network analysis, financial forensics, recommendation, and traffic forecasting (Hamilton et al., 2017b). Training GNNs has become increasingly challenging as the size of the graphs has increased rapidly. Even benchmark datasets that mimic real-life applications have grown to sizes that forbid the use of commodity laptops or servers for experimentation and model development. For example, the `MAG240M` dataset (Hu et al., 2020) has 407GB of raw data (where 349GB accounts for node features). The storage requirement easily exceeds the memory capacity of a single machine; hence, one considers either exploiting external storage or using a distributed-memory cluster. The latter imposes a natural cost barrier for many individuals and organizations, and also has been demonstrated to be often heavily communication-bound (Ramezani et al., 2022).

In this work, we exploit external storage (e.g., SSD) and perform *out-of-core* GNN training on a single machine with one or a few GPUs. Fig. 1(a) illustrates the typical memory hierarchy of such a machine. The ample external storage is assumed to be able to store the entire dataset in a format that facilitates processing and training, while the main memory cannot. Each GPU, as is common in machine architectures encountered nowadays, has an even smaller memory capacity than the main memory. We use one or multiple GPUs to perform mini-batch training.

Traditional wisdom suggests that key to the exploitation of the memory hierarchy of a machine is *locality*: *spatial locality* that takes advantage of sequential data accesses and thus reads data in blocks instead of single words, and *temporal locality*, which takes advantage of the fact that recently accessed data will be accessed again in the near future, and thus, put it at a place closer to the processors to reduce access time. In disk-based computing, for spatial locality the operating system retrieves data from disk to memory in fixed-sized 4KB to 8KB blocks, called pages. This avoids the read

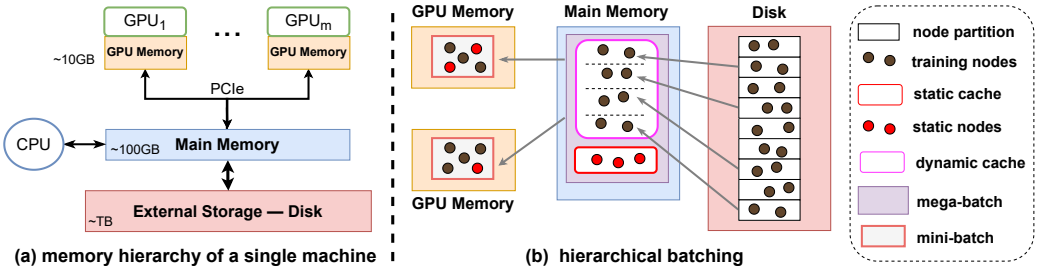

Figure 1: Overview of hierarchical batching. The disk stores the entire graph which is divided into partitions. Multiple (four in this example) partitions are randomly selected and loaded into the main memory to form a mega-batch, from which mini-batches are sampled and moved to the GPUs for training.

amplification problem (which dramatically reduces the effective disk bandwidth) when disk is read in cache-line-size blocks. For temporal locality, it is desirable that data loaded from the disk be reused as often as possible, given the significant latency caused by moving data from disk to memory.

Following this intuition, we propose a *hierarchical batching* scheme, abbreviated as HierBatching, to exploit locality in modern commodity memory hierarchy (external storage, main memory, and GPU memory). HierBatching batches data in an analogously hierarchical fashion: the entire set of graph nodes (with features and edge lists) is stored in external storage, while a *mega-batch* of nodes is sampled and copied to the main memory serving as a cache; mini-batches are then sampled from the cache for gradient-based training. We make this scheme *locality-aware* by partitioning the graph nodes into many small partitions that are stored consecutively in the disk (spatial locality), and performing mini-batch training with the same cache multiple rounds (temporal locality). HierBatching preserves the random nature of a stochastic training, as it forms each mega-batch with random combinations of partitions and samples mini-batches from the mega-batch randomly.

A realization of HierBatching incurs a subtle challenge because some of the neighbors of a node in a mega-batch may not be included in the cache, thereby degrading the training quality and the prediction accuracy. To maximally increase the node degrees with a small memory, we propose to permanently store the highest-degree nodes in the memory, because they are more likely to be connected to nodes in the mega-batch. We thus divide the main memory into a *static cache* and a *dynamic cache* and use the former to accommodate these nodes, such that their features are always reachable without repetitive transfers from the external storage. See Fig. 1(b) for a preview.

Our work makes the following contributions:

- We study a practical but under-explored scenario for training GNNs on massive graphs using external storage and propose HierBatching, a locality-aware batching scheme that fully leverages the memory hierarchy of a machine, particularly disk, to improve training efficiency.
- We introduce a static cache to compensate the loss of node degrees in the formation of the batching hierarchy, retaining model accuracy obtained by standard in-memory mini-batch training.
- We demonstrate empirically that, on a GPU equipped machine with 128GB main memory, HierBatching is **3**× to **20**× faster than DGL with `mmap` support, while retaining prediction accuracy. HierBatching is also competitive with in-memory DGL, which requires 3 times more memory.

2 Preliminaries and Related Work

In this work, we consider message-passing GNNs that act on a given graph $G(V, E)$, where V is the node set and E is the edge set. For each node $v \in V$, let $\mathbf{h}_v^0$ be the initial feature vector. A K-layer GNN uses message passing to iteratively update the feature vector and produces an output vector $\mathbf{h}_v^K$. Specifically, the update at the k-th layer ($1 \le k \le K$) reads

$$\mathbf{h}_v^k = \texttt{update}^k\Big(\mathbf{h}_v^{k-1}, \texttt{aggregate}^k\big(\{\mathbf{h}_u^{k-1} \mid u \in \mathcal{N}(v)\}\big)\Big),$$

where $\mathcal{N}(v)$ denotes the 1-hop neighborhood of v, and $\texttt{update}^k$ and $\texttt{aggregate}^k$ are operators on the feature vectors, generally layer-dependent. Common GNNs, such as GCN (Kipf & Welling,

2016), GraphSAGE (Hamilton et al., 2017a), GAT (Veličković et al., 2018), and GIN (Xu et al., 2019), follow this framework but differ in the design of the two operators.

To scale GNNs to massive datasets, a frequently studied approach is distributed-memory training (Yang, 2019; Zhang et al., 2020; Zheng et al., 2020; Jia et al., 2020; Tripathy et al., 2020; Hoang et al., 2021; Md et al., 2021; Gandhi & Iyer, 2021; Kaler et al., 2022). However, such an approach often requires frequent and voluminous inter-machine communication, including features, edge lists, models, and gradients, causing substantial challenges in parallelization, synchronization, and pipelining. LLCG (Ramezani et al., 2022) reduces communication by using local training and global correction; however, it requires a powerful global server that can process the entire graph, at odds with a limited memory budget.

GNN training is generally done by following the mini-batch training scheme, propelled by the advances in stochastic optimizations and widely adopted by the designers of neural networks. Mini-batch training on graph data, however, suffers the well-known *neighborhood explosion* problem: for a K-layer GNN, the loss of a training example requires information of its K-hop neighborhood, whose size is exponential in K in the worst case. Therefore, sampling techniques (Hamilton et al., 2017a; Chen et al., 2018; Chiang et al., 2019; Zeng et al., 2020) have been proposed to limit the size of the neighborhood. This *batching-plus-sampling* approach effectively reduces memory consumption, but data movement remains a bottleneck that hampers training efficiency. Prior work that aims at reducing data movement exists: GNS (Dong et al., 2021) employs GPU memory as a cache of main memory, loads likely-reusable data to the cache and prioritizes sampling from that data to reduce PCIe data copy; LazyGCN (Ramezani et al., 2020) recycles the already-sampled data in GPU memory, also reducing sampling and data movement overhead. However, neither approach handles the out-of-core scenario; in particular, they do not exploit spatial locality, which is critical for data stored in the disk. Marius and the sequel (Mohoney et al., 2021; Waleffe et al., 2022) are rare works that studied out-of-core training, but they employ random partitioning that compromises the partitioning quality as well as GNN prediction accuracy. Cross compared with our experiment results, to achieve a comparable accuracy, Marius++ requires several times larger a memory buffer than our cache.

Other approaches to scaling up GNNs include GNNAutoScale Fey et al. (2021), graph coarsening Huang et al. (2021), compression Liu et al. (2021), and quantization Ding et al. (2021). They are orthogonal to our approach and can be applied together with HierBatching in practice.

3 Locality-Aware Hierarchical Batching

The typical mini-batching and sampling method for training GNNs works well in the in-memory training setting, but is not efficient for the out-of-core setting. This is because the batching approach is not aware of the memory hierarchy in a real machine. More specifically, external storage accesses are much slower than memory accesses. The random nature of mini-batching causes random disk accesses, rendering out-of-core training orders of magnitude slower than in-memory training. Even if disk data is treated as a memory-mapped file (`mmap`), page alignment will inevitably cause movement of unneeded data from disk to memory. Moreover, *neighborhood sampling* can be rather inefficient, if in-memory sampling is interleaved with moving edge lists from disk to memory, hop by hop.

We thus propose HierBatching, an out-of-core scheme that effectively leverages the memory hierarchy for efficient training. The development of HierBatching undergoes a series steps, including exploiting *spatial locality* through graph partitioning (§3.1), compensating degree loss by using a *static cache* (§3.2), and improving *temporal locality* through *mega-batch reuse and pipelining* (§3.3). We summarize the overall training algorithm in §3.4 and analyze the training speedup in §3.5.

3.1 Hierarchical Batching and Spatial Locality

The first step of an efficient solution is to create a hierarchy for the batches, analogous to the memory hierarchy of a typical machine for training neural networks (external storage – main memory – GPU memory; see Fig. 1(a)). We treat the main memory as a *cache* for the disk and call data residing in the main memory a *mega-batch*. Once the mega-batch is formed through disk I/O, we may sample mini-batches from it, eliminating extra disk accesses. It has been demonstrated that if the mega-batch is sampled randomly from the entire graph, training will converge and the resulting model is as good as that trained without using mega-batches (Ramezani et al., 2020).

The solution above reduces disk accesses, but the accesses are still random. To improve *spatial locality*, we divide the nodes into *partitions* and randomly sample partitions instead of nodes to form a mega-batch. Node data of a partition, i.e., feature vectors and edge lists, are laid out contiguously in disk, so that accesses to the nodes in the same group are sequential. An obvious benefit of grouping is the reduction of random disk accesses; moreover, it leads to the I/O of more consecutive data, reducing the collateral movement of unneeded data due to page alignment. This mechanism is illustrated in Fig. 1(b), where a box denotes a partition and the dots inside are the training nodes.

The number of partitions is chosen to balance two factors: too large a partition weakens the randomness of the mega-batch, compromising training quality; too small a partition weakens spatial locality, slowing down the disk data transfer. One rule of thumb is to ensure that the edge lists of a partition occupy only a few pages, given a specific page size and the average node degree. Moreover, it is desirable to use the minimum edge cut as the partitioning objective, so that the mega-batch, as a set of partitions, loses as few neighbors as possible. For a proof of concept, we use the off-the-shelf partitioner METIS (Karypis & Kumar, 1998) in our experiments. In cases when the graph storage is beyond the memory capacity, an out-of-core partitioner is used.

3.2 Static and Dynamic Caches

Let the graph be divided into N_p disjoined partitions and the capacity of the cache (main memory) allows holding N_c ($< N_p$) partitions. In each training epoch, we randomly shuffle the partitions and move N_c partitions from the disk to perform in-memory training. The cache contains a subgraph induced by the nodes inside these N_c partitions. We enumerate mini-batches and sample neighbors for each layer from this subgraph to perform model updates. Compared with the full graph, however, such a subgraph will inevitably lose edges between the nodes in it and those outside it. This fact causes the degradation of prediction accuracy on some of the large graphs we experimented with.

To mitigate the performance loss due to insufficient neighbors, we permanently store in the memory some high-degree nodes that are helpful to increase the overall node degree. The part of the memory that holds these nodes is called the *static cache*. The rest of the memory acts as a *dynamic cache*, which holds the randomly selected partitions from the disk. As we can only allocate a small amount of memory for the static cache, we want to maximize its usage. A natural question is which static nodes are the most beneficial. Let C_S with cardinality k be the node set in the static cache and let $\{C_D^{(i)}\}$ be the node set in the dynamic cache for the i-th mega-batch. Then, the objective is to maximize the sum of increased degrees over all mega-batches:

$$\max_{C_S \subseteq V,\ |C_S|=k} \sum_i \Delta(C_D^{(i)}, C_S), \tag{1}$$

where for each mega-batch,

$$\Delta(C_D, C_S) := \sum_{u \in C_D} \sum_{v \in C_D \cup C_S} \mathbb{1}(u,v) - \sum_{u \in C_D} \sum_{v \in C_D} \mathbb{1}(u,v), \tag{2}$$

with $\mathbb{1}(u,v)$ being the indicator function which denotes the existence of an edge between nodes u and v. It is not hard to see that the solution to Eq. (1) is

$$C_S^{\text{opt}} = \{ \text{ first } k \text{ nodes } v \text{ in the decreasing order of degree}(v) - \text{degree}_{\text{sub}}(v) \ \}, \tag{3}$$

where degree(v) and degree$_{\text{sub}}(v)$ denote the degree of v in the full graph and the degree in the subgraph induced by $C_D^{(i)}$, respectively. See Appendix A for a proof.

Note that the optimal selection for the static cache derived in Eq. (3) is not "static": it depends on the content in the dynamic cache, as degree$_{\text{sub}}(v)$ changes over epochs due to the shuffling of partitions. In practice, we use degree(v) to approximate degree(v) − degree$_{\text{sub}}(v)$ when forming the static cache; that is, it contains the k nodes with the highest degrees. Inclusion of these nodes is intuitively sensible: a high-degree node connects more neighbors and offers a larger degree increase. Moreover, if all nodes have similar degrees in the subgraph as those in the full graph, then the first k nodes in the ordering of degree(v) would be similar to those in Eq. (3).

Fig. 2 illustrates the degree increase due to the use of a static cache, among nodes grouped by their degrees in the mega-batch. The orange part is the total degree increase for all nodes in the group. One sees that the group of lowest-degree nodes (0-5) incurs the most increase, benefiting the most significantly from the inclusion of static nodes; whereas the highest-degree nodes (>50) incurs the least amount of degree increase. Implementation details of the static cache are in Appendix C.1.

3.3 PIPELINING AND MEGA-BATCH REUSE

Given a mega-batch, we enumerate mini-batches of training nodes from it to perform training on GPUs. We define a "pass" as using every training node in the mega-batch exactly *once*. The data transfer from disk to form a mega-batch usually takes more time than that of executing one pass on GPUs. This means HierBatching's speed can still be limited by the disk data transfer time. On the other hand, for datasets with a low training node ratio, performing one pass may *underutilize* the data in the memory, i.e., some of the nodes in the mega-batch may not even be sampled.

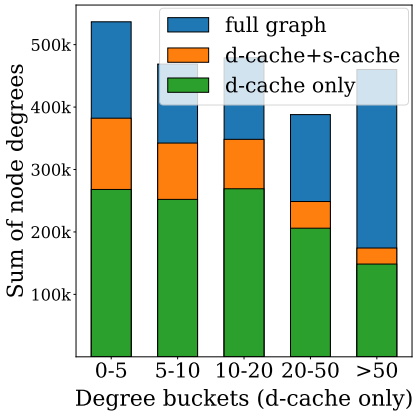

Figure 2: Node degree increase for five groups of nodes, bucketed by their degrees in the mega-batch. For each group, the green bar shows the sum of degrees before adding the static cache. The orange bar is the increase of degrees due to the inclusion of static cache, while the blue bar shows the loss of degrees.

Hence, we employ two techniques cooperatively, *pipelining* and *mega-batch reuse*, to overcome this bottleneck. The idea is to repeatedly use the *current* mega-batch in memory while waiting for the disk transfer for the *next* mega-batch, in an exchange of lowering the number of epochs required to reach training convergence. In the context of HierBatching, *pipelining* refers to overlapping the computation, i.e., training with the current mega-batch, with communication, i.e., the data transfer of the next mega-batch. In addition, *mega-batch reuse* lets the training go through a mega-batch in multiple passes to exhaust the disk transfer time for the next mega-batch. Repeated use of the mega-batch in the cache improves *temporal locality*.

Training with a mega-batch in multiple passes deviates from the usual setting of stochastic optimization. In our experiments it always converges, but its theoretical analysis is rather challenging and is beyond the scope of this paper. When done in one pass, the training is similar to ClusterGCN (Chiang et al., 2019), whose empirical success in convergence supports our proposal. On the other hand, if we are willing to assume that the mega-batches and the mini-batches therein are all sampled with replacement, the setting falls back to standard stochastic gradient descent and we do obtain convergence guarantees (Bottou et al., 2018). The challenge of analysis lies in the fact that these batches are sampled without replacement. Only very recently, analysis of such a setting was conducted and even so, it considered only strongly convex objective functions (HaoChen & Sra, 2019). We leave the analysis as future work but supplement it through empirical evidences in §4.1.

3.4 OVERALL ALGORITHM

Let us summarize the training procedure in Algorithm 1. We assume that the graph has been partitioned and each of the N_p partitions is laid out contiguously on external storage. First, fill the static cache (line 10). Then, we train in epochs (line 11), each of which performs a sweep over the entire training set. Each epoch starts with a shuffling of the partitions (line 12) and in each sub-epoch (line 13), N_d partitions from the shuffled order are loaded to main memory, forming a maga-batch (lines 14–17). This part includes loading node features and edge lists and forming the subgraph induced by the nodes in the dynamic cache and the static cache. Furthermore, this part is pipelined with the rest of the algorithm, all computations done in-memory. Therein, the mega-batch is recycled in p passes (line 19), inside each of which the training nodes are shuffled (line 20) and mini-batches are created (line 21). Then, all GPUs handle each mini-batch collectively. With q GPUs, each one gets $1/q$ of the mini-batch (lines 22–24), computes the gradient for this fraction (line 25), averages all the resulting gradients through a collective, and updates its copy of the model (line 26). The choice of the multiple input parameters for Algorithm 1 is discussed in Appendix B.

3.5 SPEEDUP ANALYSIS

We analyze the speedup of the proposed locality-aware hierarchical batching scheme, over a straightforward out-of-core training by using `mmap` without exploiting locality. We use the same notation in Algorithm 1, in which we run p passes and execute $p \times r$ mini-batches for each mega-batch. Let D be

Algorithm 1 Out-of-core GNN training with hierarchical batching (multi-GPU single-machine)

1: **Input**
2: $G(V, E)$ input graph, pre-partitioned, with nodes in the same partition stored contiguously in disk
3: N_p total number of partitions
4: C_d capacity of the dynamic cache, i.e., maximum number of nodes held in the dynamic cache
5: C_s capacity of the static cache, i.e., maximum number of nodes held in the static cache
6: B mini-batch size, i.e., number of training nodes in a mini-batch
7: p number of passes per mega-batch
8: q number of GPUs

9: Let $N_d = C_d \times N_p/|V|$ be the maximum number of partitions held in the dynamic cache.
10: Let the set of C_s highest-degree nodes be $\mathcal{P}$. Move the features of $\mathcal{P}$ to the main memory. ▷ static cache
11: **for each** epoch **do**
12: τ = random.permutation(n) ▷ shuffle the partitions in disk
13: **for each** $i \in [0, \frac{N_p}{N_d})$ **do** ▷ hierarchical batching at the main memory level
▷ lines 14–17 are pipelined with lines 18–26

14: Let the set of nodes in partitions $\tau[i \times N_d],\ \tau[i \times N_d + 1],\ \ldots,\ \tau[(i+1) \times N_d - 1]$ be $\mathcal{T}$
15: Move the features of $\mathcal{T}$ to the dynamic cache in the main memory ▷ disk data transfer
16: Move the edge lists of $\mathcal{T} \cup (\mathcal{N}(\mathcal{T}) \cap \mathcal{P})$ to the main memory ▷ $\mathcal{N}(\mathcal{T})$ is $\mathcal{T}$'s neighborhood
17: Form a subgraph $\mathcal{G}_{cache}$ with node set $\mathcal{T} \cup (\mathcal{N}(\mathcal{T}) \cap \mathcal{P})$ ▷ a new mega-batch formed

18: Let $S_{\mathcal{T}}$ be the number of training nodes in $\mathcal{T}$, and $r = \frac{S_{\mathcal{T}}}{B}$ be the number of mini-batches per pass
19: **for each** pass $j \in [1, p]$ **do** ▷ reuse data in main memory
20: Shuffle training nodes in $\mathcal{G}_{cache}$ into GPU-level mini-batches $\{\mathcal{B}_1, \ldots, \mathcal{B}_{q \times r}\}$
21: **for each** mini-batch $k \in [0, r)$ **do** ▷ hierarchical batching at the GPU level
22: **for each** GPU $d \in [1, q]$ **in parallel do** ▷ multi-GPU training
23: Sample a message-flow graph $\mathcal{G}_s$ from $\mathcal{G}_{cache}$ for the mini-batch $\mathcal{B}_{k \times q + d}$
24: Move $\mathcal{G}_s$ to the GPU memory
25: Evaluate the model (forward) and compute the gradient (backward)
26: All GPUs average the gradient and update the model

the node feature dimension and S_{feat} be the data precision in bytes. Let BW_{seq} and BW_{rand} be the disk bandwidth when performing sequential accesses and random accesses, respectively. Generally, $BW_{rand}/BW_{seq} := \alpha \approx S_{acc}/S_{opt}$, where $S_{acc} = D \times S_{feat}$ is the size of a single random access and S_{opt} is the optimal disk request size that leads to sequential access. For example, in the MAG240M dataset, $D = 768$ and $S_{feat} = 2$B, while $S_{opt} = 4$KB for a modern flash disk. Then, $\alpha = 768 \times 2/4069 = 0.375$, which means that random access of a node feature vector leverages only 37.5% of the peak disk bandwidth.

For simplicity of analysis, we neglect the disk transfer of the graph, as loading node features is way more time consuming for large D. Using `mmap` without locality, the time to load one mini-batch is $t_{disk}^{mini} = B \times F \times D \times S_{feat}/BW_{rand}$, where B is the mini-batch size and F is the sampling fanout. Let γ be the ratio of training nodes in the graph, and we assume even distribution of training nodes across mega-batches, so that $S_{\mathcal{T}}/C_d \approx \gamma$. Let the time to train one mini-batch be t_{gpu}, which includes data transfer from memory to GPUs, doing forward and backward calculations, averaging gradients, and updating the model. Typically, $t_{disk}^{mini}/t_{gpu} := \beta > 1$. Assuming pipelining, the majority time to train $p \times r$ mini-batches is $t_{mmap} = p \times r \times t_{disk}^{mini}$. On the other hand, for HierBatching, loading one mega-batch takes time $t_{disk}^{mega} = C_d \times D \times S_{feat}/BW_{seq}$ and thus training takes time $t_{hier} = \max\{t_{disk}^{mega}, p \times r \times t_{gpu}\}$. Therefore, the speedup is $t_{mmap}/t_{hier} = p \times \gamma \times F/\alpha$ if disk access takes more time in HierBatching; otherwise, $t_{mmap}/t_{hier} = \beta$.

4 Evaluation

Datasets and evaluation metric. We use large benchmark datasets listed in Table 1. Mag240M and ogbn-* datasets come from the Open Graph Benchmark Hu et al. (2020; 2021). Mag240M-C is the subgraph extracted from Mag240M that contains only paper citation edges. All graphs are made

undirected if they are originally not. The data statistics after the transformation are listed in Table 1. On each dataset, the task is to predict node labels. Although smaller datasets such as ogbn-arxiv and ogbn-products could easily fit into the main memory in our setting, they are included in the evaluation to demonstrate the competitive model quality produced by HierBatching.

Table 1: Summary of evaluated datasets

Dataset	# Nodes	# Edges	Feature	Classes	Multi-label	Train / Val / Test	Raw data size
ogbn-arxiv	169,343	2,332,486	128	40	No	0.54 / 0.18 / 0.29	123MB
ogbn-products	2,449,029	123,718,024	100	47	No	0.08 / 0.02 / 0.90	2.8GB
ogbn-papers100M	111,059,956	3,231,371,744	128	172	No	0.01 / 0.001 / 0.002	**103GB**
Mag240M-C	121,751,666	2,595,497,852	768	153	No	0.01 / 0.001 / 0.001	**214GB**
Mag240M	244,160,499	3,456,728,464	768	153	No	4.5e-3 / 6e-4 / 6e-4	**407GB**

Evaluation platform. We use two compute platforms in our experiments, a local cluster and AWS. Each compute node in the local cluster has 32 CPU cores, 1TB DRAM and 4 NVIDIA V100 GPUs. The AWS instance has 24 CPU cores (2-way hyperthreading, 48 threads), 386GB DRAM and 4 NVIDIA T4 GPUs. The AWS machine is equipped with a fast local flash storage while the local cluster stores the datasets in a networked file system. The difference of the two is useful in showing how I/O throughputs could affect training speed. We regulate the DRAM size on both platforms, e.g., from 128GB to 386GB, to meet the memory budget assumptions of different experiments.

Experimental Setup. We implement HierBatching based on PyTorch Paszke et al. (2019) and DGL Wang et al. (2019). We use the *micro F1-score* to measure accuracy. For accuracy-related experiments, we run the training for a fixed number of epochs as listed in Table 4 in the Appendix. We report the test scores produced by the model at the best validation epoch during the training. To obtain the training time per epoch, we run each experiment for five epochs and take an average. Further details of our experimental settings are deferred to Appendix C.

4.1 Accuracy Comparison with Standard Neighborhood Sampling

To demonstrate that HierBatching retains the accuracy of standard in-memory training schemes, we compare test accuracy of HierBatching (`HB`) with that of *neighbor sampling* (`NS`), the standard mini-batching and sampling method used to train large-scale GNNs (Hamilton et al., 2017a). `NS` assumes full graph accesses during sampling. We allocate as much memory as `NS` needs to run in memory. For `HB`, we choose static cache capacity $C_s = |V|/100$ and number of passes $p = 2$. For a given dataset and model, we keep common hyper-parameters the same (e.g. GNN layers, hidden dimensions, learning rates) across all methods. Detailed hyper-parameter settings are in Appendix C.

Table 2 lists the test F1-micro scores obtained by `NS` and `HB`. We observe that their resulting accuracies are nearly the same across models and datasets. However, without the static cache, `HB(-s)` suffers notable accuracy degradation ($\geq$1%) in many cases, as shown in red. This observation demonstrates the importance of static cache for HierBatching. We also observe that `HB` and the no mega-batch reuse version, `HB(-r)`, achieve a similar accuracy, which means that mega-batch reuse does not compromise the training quality. Note that similarly to `HB(-s)`, Marius++ also suffers accuracy degradation (Waleffe et al., 2022), as it does random partitioning without compensating edge loss. We conduct a comparison with Marius++ in Appendix D.1.

4.2 Convergence Rates and Training Time

Fig. 3 shows the model convergence in terms of epochs, for both `NS` and `HB` approaches. We observe that without the static cache, `HB(-s)` not only lowers final accuracy but converges at a much slower rate, while `HB(-r)` converges almost as fast as `NS`. Even though we follow a non-standard stochastic training approach in `HB` by reusing each mega-batches, the model still converges well and in some cases even faster than `NS` (e.g., ogbn-products), primarily because it perform twice as many gradient updates per epoch. More gradient updates do not necessarily translate into longer training time in `HB` since the system is bottlenecked by I/O, not gradient computation. As we will show immediately, the training time per epoch in `HB` is very much comparable to the in-memory `NS` approach.

We compare the training speed of HierBatching with two settings of DGL, DGL* and DGL+`mmap`. DGL* is the vanilla DGL which requires all data to be resident in the memory. It uses 386GB main

Table 2: Comparison of test accuracies (F1-micro score) between HierBatching (HB) and neighbor sampling (NS). HB uses $C_s = |V|/100$ and $p = 2$. HB (-s) disables the static cache on top of HB, i.e., $C_s = 0$. HB (-r) disables mega-batch reuse on top of HB, i.e., $p = 1$. Significant accuracy drops are hignlighted in red.

GNN Model	Dataset	NS	HB (-s)	HB (-r)	HB
SAGE	ogbn-arxiv	71.52	70.99	71.43	71.42
	ogbn-products	78.90	78.98	78.90	78.84
	ogbn-papers100M	64.94	63.85	64.56	64.83
	Mag240M-C	65.92	64.94	65.69	65.98
	Mag240M	68.83	67.08	68.25	68.56
GAT	ogbn-arxiv	71.76	69.58	71.21	71.73
	ogbn-products	79.54	79.61	79.58	79.55
	ogbn-papers100M	64.58	61.45	64.31	64.20
	Mag240M-C	65.74	65.06	65.69	66.09
	Mag240M	68.40	67.33	68.07	68.89
GIN	ogbn-arxiv	70.24	68.61	70.22	70.10
	ogbn-products	75.70	76.58	76.15	76.77
	ogbn-papers100M	65.07	62.33	64.63	64.81
	Mag240M-C	63.73	62.93	63.59	63.36
	Mag240M	67.47	66.33	67.02	66.58

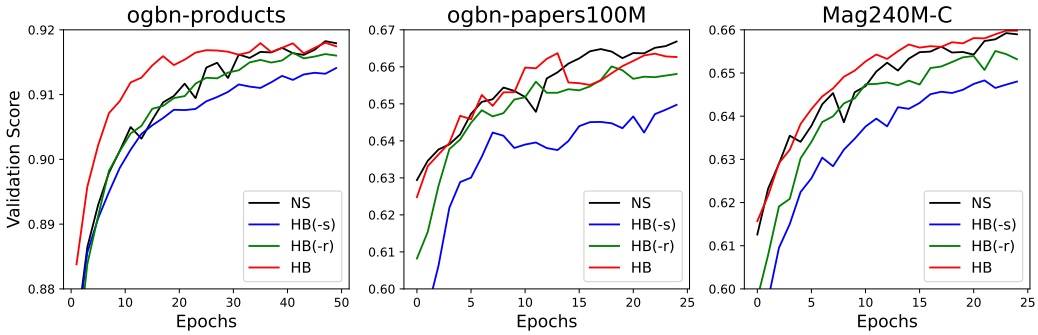

Figure 3: GraphSAGE convergence history for neighbor sampling and HierBatching.

memory. DGL+mmap adds the mmap [1] support on top of DGL to handle the case of insufficient main memory. This setting uses 128GB main memory.

Table 3 lists the training time per epoch on the AWS machine. The first observation is that HierBatching (HB) can run all of the cases, thanks to HierBatching's awareness of the memory hierarchy. In contrast, DGL runs out of memory for the largest dataset, Mag240M, which requires 349GB space to accommodate the feature data and 135GB for the graph structures (DGL maintains all three COO, CSC and CSR formats in memory). Even with mmap support, DGL+mmap can not run Mag240M within the limited memory budget, since it fails to hold the graph structures in memory.

The second observation is, HB runs significantly faster than mmap, and is only slightly slower than in-memory training. Compared with DGL+mmap, HierBatching achieves 2.6× to 20.4× speedup across different datasets and models (4.3× on average), mainly because of the improved spatial locality. As shown in §3.5, speedup depends on training nodes ratio γ and fanout F, thus speedups vary across different datasets. Compared to DGL*, The training HierBatching can achieve competitive training speed with a maximum slowdown of 41% (GIN on mag240M-C), even though HierBatching has only one third of the memory capacity! Surprisingly, for some cases, e.g., GIN on ogbn-papers100M, HB is faster than DGL*. It turns out that these cases are GPU compute bound, and HB usually has smaller sampled graphs than DGL*, which means less GPU computation. Overall, these results demonstrate that HierBatching is extremely efficient in taking advantage of the system resources.

Notice that the AWS instance has a faster storage than the local cluster. We show the training time per epoch on the the local cluster in Table 6 in Appendix D. Due to slower network-based storage

[1] We use the PyTorch API `torch.Storage.from_file` to create mmap-ed tensors. It is infeasible to mmap graph structure data without significant modifications to the DGL codebase. Thus, we only mmap node features.

Table 3: Comparison of training time (sec) per epoch between HierBatching (HB), DGL* and DGL+`mmap`, on the **AWS** machine. DGL* uses 386GB memory, while HB and DGL+`mmap` use 128GB memory.

Dataset	SAGE			GAT			GIN		
	DGL*	DGL+`mmap`	HB	DGL*	DGL+`mmap`	HB	DGL*	DGL+`mmap`	HB
ogbn-papers100M	202.6	1017.8	278.0	382.3	1426.3	385.8	822.2	9131.6	448.0
Mag240M-C	178.6	678.3	249.4	379.9	1042.7	326.9	183.5	664.6	258.3
Mag240M	OoM	OoM	521.3	OoM	OoM	546.6	OoM	OoM	528.3

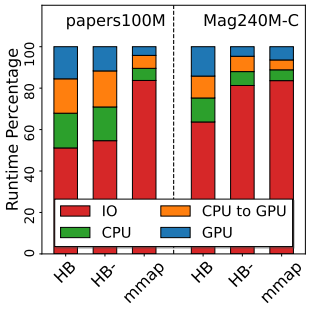

Figure 4: Training time breakdown. Pipelining is disabled to better illustrate the overhead of each components.

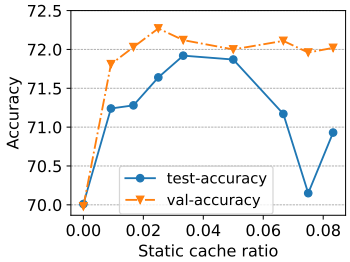

(a) ogbn-arxiv

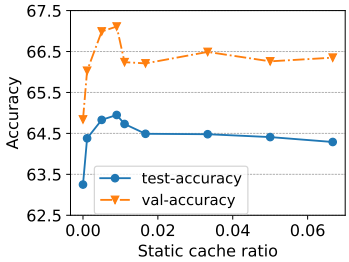

(b) ogbn-papers100M

Figure 5: Trade-off on static and dynamic cache sizes. 'Static cache ratio' refers to $C_s/|V|$. The overall budget for dynamic cache and static cache is $|V| \times 1\%$.

system, we observe even larger speedup (up to 58×) of HierBatching over DGL+`mmap`. Note that this network-based storage architecture is quite common in modern datacenters and supercomputing centers, which means HierBatching will be quite useful in the real systems.

4.3 Ablation Study and Sensitivity Study

In order to study the influence of spatial locality, we disrupt `HB`'s feature contiguous layout in disk, denoted as `HB-`, which thus access node features randomly and can not enjoy spatial locality. `HB-` differs from DGL+`mmap` as it forms mega-batches in memory. Fig. 4 reports the training time breakdown of three approaches. Interestingly, `HB-` exhibits different behaviors with two datasets. For ogbn-papers100M where the node feature size is relatively small, `HB-` allows the operating system to cache most of the feature data in the memory as training proceeds and yields almost no slowdown. This is not possible with DGL+`mmap` since the full graph structure takes almost all the available memory space, leaving little space for caching. In contrast, the node feature size of Mag240M-C far exceeds the memory budget and cannot be cached efficiently. In this case, `HB-` behaves very similarly with DGL+`mmap`, spending most of the time on gathering node features from the external storage.

Given a certain memory budget, the static cache capacity C_s and dynamic cache capacity C_d are two competing parameters. Increasing C_s can keep more high-degree nodes in the memory, but also decreases C_d and thus reduces randomness. Oppositely, increasing C_d increases randomness but reduces the degrees compensation by the static cache. We conduct an experiment with a fixed memory quota for dynamic cache and static cache, and study how the accuracy changes as the static cache ratio changes in Fig. 5. As shown, all curves in both figures peak at a static cache ratio between $(0, 0.04)$, which demonstrates that there does exist a sweet spot to pick the sizes of the two caches.

5 Conclusions

We have proposed a novel locality-aware GNN training approach, HierBatching, for scaling up GNNs to massive graphs. HierBatching targets a single machine with multiple GPUs but a limited memory budget. The core of our approach is hierarchical batching, which hierarchically divides the training data to match the memory hierarchy of the machine. The main memory serves as a cache for the disk, and is fully utilized as a dynamic cache and a static cache, to balance training speed and prediction quality. Overall, our approach effectively improves both spatial and temporal locality. Experiment results demonstrate that HierBatching dramatically improves GNN training speed for massive graphs on a single machine, while retaining the prediction accuracy.

REPRODUCIBILITY STATEMENT

We provide a link to an ananymous Github repository hosting the code, scripts and instructions to reproduce results in our evaluation section: https://github.com/HierBatching/HierBatching. Detailed instructions on how to prepare the datasets, build and run the code are included in the `README.txt` file under the repository.

REFERENCES

Léon Bottou, Frank E. Curtis, and Jorge Nocedal. Optimization methods for large-scale machine learning. *SIAM Review*, 60(2):223–311, 2018.

Jie Chen, Tengfei Ma, and Cao Xiao. FastGCN: Fast learning with graph convolutional networks via importance sampling. In *International Conference on Learning Representations*, 2018. URL https://openreview.net/forum?id=rytstxWAW.

Wei-Lin Chiang, Xuanqing Liu, Si Si, Yang Li, Samy Bengio, and Cho-Jui Hsieh. Cluster-gcn: An efficient algorithm for training deep and large graph convolutional networks. In *Proceedings of the 25th ACM SIGKDD International Conference on Knowledge Discovery & Data Mining*, KDD '19, pp. 257–266, New York, NY, USA, 2019. Association for Computing Machinery. ISBN 9781450362016. doi: 10.1145/3292500.3330925. URL https://doi.org/10.1145/3292500.3330925.

Mucong Ding, Kezhi Kong, Jingling Li, Chen Zhu, John Dickerson, Furong Huang, and Tom Goldstein. Vq-gnn: A universal framework to scale up graph neural networks using vector quantization. *Advances in Neural Information Processing Systems*, 34:6733–6746, 2021.

Jialin Dong, Da Zheng, Lin F. Yang, and George Karypis. Global neighbor sampling for mixed cpu-gpu training on giant graphs. In *Proceedings of the 27th ACM SIGKDD Conference on Knowledge Discovery & Data Mining*, KDD '21, pp. 289–299, New York, NY, USA, 2021. Association for Computing Machinery. ISBN 9781450383325. doi: 10.1145/3447548.3467437. URL https://doi.org/10.1145/3447548.3467437.

Matthias Fey, Jan E Lenssen, Frank Weichert, and Jure Leskovec. Gnnautoscale: Scalable and expressive graph neural networks via historical embeddings. In *International Conference on Machine Learning*, pp. 3294–3304. PMLR, 2021.

Swapnil Gandhi and Anand Padmanabha Iyer. P3: Distributed deep graph learning at scale. In *15th USENIX Symposium on Operating Systems Design and Implementation (OSDI 21)*, pp. 551–568. USENIX Association, July 2021. ISBN 978-1-939133-22-9. URL https://www.usenix.org/conference/osdi21/presentation/gandhi.

William L. Hamilton, Rex Ying, and Jure Leskovec. Inductive representation learning on large graphs. In *Proceedings of the 31st International Conference on Neural Information Processing Systems*, NIPS '17, pp. 1025–1035, Red Hook, NY, USA, 2017a. Curran Associates Inc. ISBN 9781510860964.

William L Hamilton, Rex Ying, and Jure Leskovec. Representation learning on graphs: Methods and applications. *arXiv preprint arXiv:1709.05584*, 2017b.

Jeff HaoChen and Suvrit Sra. Random shuffling beats SGD after finite epochs. In *ICML*, 2019.

Loc Hoang, Xuhao Chen, Hochan Lee, Roshan Dathathri, Gurbinder Gill, and Keshav Pingali. Efficient Distribution for Deep Learning on Large Graphs. In *Proceedings of the Workshop on Graph Neural Networks and Systems*, 2021. URL https://chenxuhao.github.io/docs/gnnsys-2021.pdf.

Weihua Hu, Matthias Fey, Marinka Zitnik, Yuxiao Dong, Hongyu Ren, Bowen Liu, Michele Catasta, and Jure Leskovec. Open graph benchmark: Datasets for machine learning on graphs. In H. Larochelle, M. Ranzato, R. Hadsell, M. F. Balcan, and H. Lin (eds.), *Advances in Neural Information Processing Systems*, volume 33, pp. 22118–22133. Curran Associates, Inc., 2020. URL https://proceedings.neurips.cc/paper/2020/file/fb60d411a5c5b72b2e7d3527cfc84fd0-Paper.pdf.

Weihua Hu, Matthias Fey, Hongyu Ren, Maho Nakata, Yuxiao Dong, and Jure Leskovec. Ogb-lsc: A large-scale challenge for machine learning on graphs. *arXiv preprint arXiv:2103.09430*, 2021.

Zengfeng Huang, Shengzhong Zhang, Chong Xi, Tang Liu, and Min Zhou. Scaling up graph neural networks via graph coarsening. In *Proceedings of the 27th ACM SIGKDD Conference on Knowledge Discovery & Data Mining*, pp. 675–684, 2021.

Zhihao Jia, Sina Lin, Mingyu Gao, Matei Zaharia, and Alex Aiken. Improving the accuracy, scalability, and performance of graph neural networks with roc. In *Proceedings of the 3rd Conference on Machine Learning and Systems (MLSys)*, March 2020.

Tim Kaler, Nickolas Stathas, Anne Ouyang, Alexandros-Stavros Iliopoulos, Tao Schardl, Charles E. Leiserson, and Jie Chen. Accelerating training and inference of graph neural networks with fast sampling and pipelining. In D. Marculescu, Y. Chi, and C. Wu (eds.), *Proceedings of Machine Learning and Systems*, volume 4, pp. 172–189, 2022. URL https://proceedings.mlsys.org/paper/2022/file/35f4a8d465e6e1edc05f3d8ab658c551-Paper.pdf.

George Karypis and Vipin Kumar. A fast and high quality multilevel scheme for partitioning irregular graphs. *SIAM Journal on scientific Computing*, 20(1):359–392, 1998.

Thomas Kipf and Max Welling. Semi-supervised classification with graph convolutional networks. In *International Conference on Learning Representations*, ICLR '16, 2016.

Zirui Liu, Kaixiong Zhou, Fan Yang, Li Li, Rui Chen, and Xia Hu. Exact: Scalable graph neural networks training via extreme activation compression. In *International Conference on Learning Representations*, 2021.

Vasimuddin Md, Sanchit Misra, Guixiang Ma, Ramanarayan Mohanty, Evangelos Georganas, Alexander Heinecke, Dhiraj Kalamkar, Nesreen K. Ahmed, and Sasikanth Avancha. DistGNN: Scalable distributed training for large-scale graph neural networks. In *Proceedings of the International Conference for High Performance Computing, Networking, Storage and Analysis*, SC '21, New York, NY, USA, 2021. Association for Computing Machinery. ISBN 9781450384421. doi: 10.1145/3458817.3480856. URL https://doi.org/10.1145/3458817.3480856.

Jason Mohoney, Roger Waleffe, Henry Xu, Theodoros Rekatsinas, and Shivaram Venkataraman. Marius: Learning massive graph embeddings on a single machine. In *15th USENIX Symposium on Operating Systems Design and Implementation (OSDI 21)*, pp. 533–549. USENIX Association, July 2021. ISBN 978-1-939133-22-9. URL https://www.usenix.org/conference/osdi21/presentation/mohoney.

Adam Paszke, Sam Gross, Francisco Massa, Adam Lerer, James Bradbury, Gregory Chanan, Trevor Killeen, Zeming Lin, Natalia Gimelshein, Luca Antiga, Alban Desmaison, Andreas Kopf, Edward Yang, Zachary DeVito, Martin Raison, Alykhan Tejani, Sasank Chilamkurthy, Benoit Steiner, Lu Fang, Junjie Bai, and Soumith Chintala. Pytorch: An imperative style, high-performance deep learning library. In H. Wallach, H. Larochelle, A. Beygelzimer, F. d'Alché-Buc, E. Fox, and R. Garnett (eds.), *Advances in Neural Information Processing Systems 32*, pp. 8026–8037. Curran Associates, Inc., 2019. URL http://papers.nips.cc/paper/9015-pytorch-an-imperative-style-high-performance-deep-learning-library.pdf.

Morteza Ramezani, Weilin Cong, Mehrdad Mahdavi, Anand Sivasubramaniam, and Mahmut Kandemir. Gcn meets gpu: Decoupling "when to sample"from "how to sample". In H. Larochelle, M. Ranzato, R. Hadsell, M.F. Balcan, and H. Lin (eds.), *Advances in Neural Information Processing Systems*, volume 33, pp. 18482–18492. Curran Associates, Inc., 2020. URL https://proceedings.neurips.cc/paper/2020/file/d714d2c5a796d5814c565d78dd16188d-Paper.pdf.

Morteza Ramezani, Weilin Cong, Mehrdad Mahdavi, Mahmut T Kandemir, and Anand Sivasubramaniam. Learn locally, correct globally: A distributed algorithm for training graph neural networks. In *The International Conference on Learning Representations*, 2022.

Alok Tripathy, Katherine Yelick, and Aydın Buluç. Reducing communication in graph neural network training. In *Proceedings of the International Conference for High Performance Computing, Networking, Storage and Analysis*, SC '20. IEEE Press, 2020. ISBN 9781728199986.

Petar Veličković, Guillem Cucurull, Arantxa Casanova, Adriana Romero, Pietro Liò, and Yoshua Bengio. Graph attention networks. In *International Conference on Learning Representations*, ICLR '18, 2018. URL https://openreview.net/forum?id=rJXMpikCZ.

Roger Waleffe, Jason Mohoney, Theodoros Rekatsinas, and Shivaram Venkataraman. Marius++: Large-scale training of graph neural networks on a single machine. *CoRR*, abs/2202.02365, 2022. URL https://arxiv.org/abs/2202.02365.

Minjie Wang, Lingfan Yu, Da Zheng, Quan Gan, Yu Gai, Zihao Ye, Mufei Li, Jinjing Zhou, Qi Huang, Chao Ma, Ziyue Huang, Qipeng Guo, Hao Zhang, Haibin Lin, Junbo Zhao, Jinyang Li, Alexander J. Smola, and Zheng Zhang. Deep graph library: Towards efficient and scalable deep learning on graphs. In *International Conference on Learning Representations*, ICLR '19, 2019.

Keyulu Xu, Weihua Hu, Jure Leskovec, and Stefanie Jegelka. How powerful are graph neural networks? In *International Conference on Learning Representations*, ICLR '19, 2019. URL https://openreview.net/forum?id=ryGs6iA5Km.

Hongxia Yang. Aligraph: A comprehensive graph neural network platform. In *Proceedings of the 25th ACM SIGKDD International Conference on Knowledge Discovery & Data Mining*, KDD '19, pp. 3165–3166, New York, NY, USA, 2019. Association for Computing Machinery. ISBN 9781450362016. doi: 10.1145/3292500.3340404. URL https://doi.org/10.1145/3292500.3340404.

Hanqing Zeng, Hongkuan Zhou, Ajitesh Srivastava, Rajgopal Kannan, and Viktor Prasanna. Graph-saint: Graph sampling based inductive learning method. In *International Conference on Learning Representations*, 2020. URL https://openreview.net/forum?id=BJe8pkHFwS.

Dalong Zhang, Xin Huang, Ziqi Liu, Jun Zhou, Zhiyang Hu, Xianzheng Song, Zhibang Ge, Lin Wang, Zhiqiang Zhang, and Yuan Qi. Agl: A scalable system for industrial-purpose graph machine learning. *Proc. VLDB Endow.*, 13(12):3125–3137, Aug 2020. ISSN 2150-8097. doi: 10.14778/3415478.3415539. URL https://doi.org/10.14778/3415478.3415539.

Da Zheng, Chao Ma, Minjie Wang, Jinjing Zhou, Qidong Su, Xiang Song, Quan Gan, Zheng Zhang, and George Karypis. DistDGL: Distributed graph neural network training for billion-scale graphs, 2020.

A PROOF OF EQ. (3)

Simplifying Eq. (2), we obtain

$$\begin{aligned}\Delta(C_D, C_S) &= \sum_{u \in C_D} \sum_{v \in C_S \setminus C_D} \mathbb{1}(u, v) \\ &= \sum_{u \in C_D} \left(\sum_{v \in C_S} \mathbb{1}(u, v) - \sum_{v \in C_D \cap C_S} \mathbb{1}(u, v) \right) \\ &= \sum_{v \in C_S} \sum_{u \in C_D} \mathbb{1}(u, v) - \sum_{v \in C_D \cap C_S} \sum_{u \in C_D} \mathbb{1}(u, v).\end{aligned} \tag{4}$$

Define the partition assignment function f: $f(v) = i \iff v \in C_D^{(i)}$. Then, by substituting $\Delta(C_D^{(i)}, C_S)$ with Eq. (4) in Eq. (1), it follows that

$$\begin{aligned}\sum_i \Delta(C_D^{(i)}, C_S) &= \sum_i \left(\sum_{v \in C_S} \sum_{u \in C_D^{(i)}} \mathbb{1}(u, v) - \sum_{v \in C_D^{(i)} \cap C_S} \sum_{u \in C_D^{(i)}} \mathbb{1}(u, v) \right) \\ &= \sum_{v \in C_S} \sum_i \sum_{u \in C_D^{(i)}} \mathbb{1}(u, v) - \sum_i \sum_{v \in C_D^{(i)} \cap C_S} \sum_{u \in C_D^{(f(v))}} \mathbb{1}(u, v) \\ &= \sum_{v \in C_S} \sum_{u \in V} \mathbb{1}(u, v) - \sum_{v \in C_S} \sum_{u \in C_D^{(f(v))}} \mathbb{1}(u, v) \\ &= \sum_{v \in C_S} \left(\text{degree}(v) - \text{degree}_{\text{sub}}(v) \right).\end{aligned} \tag{5}$$

Therefore, to maximize Eq. (5) with a cache budget k, we sort all nodes in V according to $\text{degree}(v) - \text{degree}_{\text{sub}}(v)$ and take the first k nodes.

B CHOICE OF PARAMETERS IN ALGORITHM 1

Assume that the main memory size is X bytes and the memory size of a single GPU is Y bytes. The choice of the mini-batch size B, in part, depends on Y for a maximal GPU utilization. Meanwhile, B affects convergence and training quality and thus is an important hyperparameter for tuning.

Assume that $S_p = \frac{|V|}{N_p}$ is the size of a single partition, D is the node feature dimension, S_{feat} is the data precision in bytes, and S_{opt} is the optimal disk request size that leads to sequential access. We choose S_p to be no less than $S_{opt}/(D \times S_{feat})$, such that disk accesses are sequential. Hence, N_p is no greater than $|V| \times D \times S_{feat}/S_{opt}$.

Given a fixed X, increasing the dynamic cache size will decrease the static cache size. Hence, the static cache capacity C_s and the dynamic cache capacity C_d are faced with a trade off. If the dataset has A GB feature data and B GB edge list data, the minimum memory size required for HierBatching to work properly is $[2r_s \times A + 2r_d \times (A + B)]$ GB, where $r_s = C_s/|V|$, $r_d = C_d/|V|$, and the factor 2 comes from double buffering required for pipelining. Typical values of r_s and r_d in our experiments are $r_s = 0.01$ and $r_d \in [0.0625, 0.25]$.

The number of passes p tradeoffs between convergence speed and accuracy. It is an important tuning hyperparameter.

C EVALUATION DETAILS

C.1 IMPLEMENTATION DETAILS

Since static nodes are high-degree nodes, their edge lists may be too large to stay in the main memory, especially for power-law graphs. As a trade-off, only the features of the static nodes are stored in

the cache, while the edge lists are kept in the disk. Because the static nodes are scattered in the disk, we store another copy of the edge lists for them in the disk contiguously, so that disk accesses remain sequential when edge lists are moved to the memory at every reloading of the dynamic cache (i.e., forming a new mega-batch). While loading edge lists, we only keep the edges of the induced subgraph of the mega-batch in memory, which needs much less memory space.

C.2 Clarification of Datasets

The complete Mag240M dataset is a heterogeneous academic graph on which a relational GNN model would work the best. For ease of implementation, in the evaluation we treat it as a homogeneous graph and apply non-relational GNN models instead. Only minor accuracy drops are observed when compared with relational GNN baselines posted on OGB-LSC benchmark Hu et al. (2021). For datasets without publicly available test sets (Mag240M-C, Mag240M), we report the highest validation F1-scores. Considering the scales of large datasets, test and validation are performed with minibatching and sampling, similar to the practice in Kaler et al. (2022).

C.3 Hyper-parameter Settings

Table 4 lists the key hyper-parameters we use in our experiment. Note that when evaluating the training speed, we use the same hyper-parameters, except that GAT uses hidden size of 512 in Table 3, but 1024 in Table 2 due to the smaller GPU memory on the AWS instance.

Table 4: Training configurations for results in Table 2

Dataset	**SAGE**					
	Epochs	Hidden	Learning rate	Dropout	Fanouts	Layers
ogbn-arxiv	100	256	0.001	0.5	(15,10,5) / (50,50,50)	3
ogbn-products	50	256	0.001	0.5	(15,10,5) / (20,20,20)	3
ogbn-papers100M	25	256	0.001	0.5	(15,10,5) / (20,20,20)	3
Mag240M-C	25	1024	0.001	0.5	(25,15) / (25,15)	2
Mag240M	25	1024	0.001	0.5	(25,15) / (25,15)	2
Dataset	**GAT**					
	Epochs	Hidden	Learning rate	Dropout	Fanouts	
ogbn-arxiv	100	256	0.001	0.5	(15, 10, 5) / (50,50,50)	3
ogbn-products	50	512	0.001	0.5	(15, 10, 5) / (20,20,20)	3
ogbn-papers100M	25	1024	0.001	0.5	(15, 10, 5) / (20,20,20)	3
Mag240M-C	25	1024	0.001	0.5	(25,15) / (25,15)	2
Mag240M	25	1024	0.001	0.5	(25,15) / (25,15)	2
Dataset	**GIN**					
	Epochs	Hidden	Learning rate	Dropout	Fanouts	
ogbn-arxiv	100	128	0.001	0.5	(20,20,20) / (20,20,20)	3
ogbn-products	50	512	0.003	0.5	(15,10,5) / (20,20,20)	3
ogbn-papers100M	25	512	0.003	0.5	(20,20,20) / (20,20,20)	3
Mag240M-C	25	1024	0.001	0.5	(25,15) / (25,15)	2
Mag240M	25	1024	0.001	0.5	(25,15) / (25,15)	2

Table 5 shows some extra parameters for HierBatching. N_p is the total number of partitions. N_d is the maximum number of partitions held in the dynamic cache. $r_s = C_s/|V|$ is the ratio of nodes kept in the static cache. p is the number of passes per mega-batch.

Table 5: Extra training configurations for HierBatching in Table 2

Dataset	N_p	N_d	r_s	p
ogbn-arxiv	1024	256	0.01	2
ogbn-products	4096	512	0.01	2
ogbn-papers100M	16384	1024	0.01	2
Mag240M-C	16384	1024	0.01	2
Mag240M	16384	1024	0.01	2

D ADDITIONAL EXPERIMENTS

Table 6 shows the training time per epoch on the local cluster. As it has faster GPUs (V100), its in-memory training, i.e., DGL*, is faster than that on the AWS machine. However, since it uses a network-based storage system, its random access latency is significantly larger than that of the AWS machine. Consequently, the DGL+`mmap` setting performs dramatically worse than that on AWS. In comparison, HierBatching (`HB`) becomes faster than that on AWS, as the storage system in the local cluster has similar sequential IO throughput as that of AWS, and `HB` can fully enjoy fast sequential accesses, thanks to the spatial locality aware design.

Table 6: Comparison of training time (s) per epoch between HierBatching (HB), DGL* and DGL+`mmap` on the **local cluster**. DGL* uses 386GB memory, while HB and DGL+`mmap` use 128GB memory. TO: timeout (>5 hours).

Dataset	SAGE			GAT			GIN		
	DGL*	DGL+mmap	HB	DGL*	DGL+mmap	HB	DGL*	DGL+mmap	HB
ogbn-papers100M	105.4	11037.5	190.3	254.2	11850.3	260.7	348.7	TO	238.8
Mag240M-C	77.7	TO	229.1	142.3	TO	185.8	75.7	TO	193.7
Mag240M	OoM	OoM	1708.3	OoM	OoM	1828.5	OoM	OoM	1788.9

D.1 CROSS COMPARISON WITH MARIUS++

When cross compared with our experimental results, to achieve an acceptable accuracy Marius++ requires a much larger cache/buffer than HierBatching does. For example, for ogbn-papers100M on SAGE, Marius++ keeps 7/16 of overall data in memory, achieving 66.03% validation accuracy, while HierBatching only loads $2\times1/16$ of the data but achieves 66.42% (`random` partitioning) and 67.03% (`METIS` partitioning) validation accuracy.